Received: 30 November 2023 | Revised: 26 April 2024 | Accepted: 27 April 2024

DOI: 10.1002/mp.17172

RESEARCH ARTICLE

MEDICAL PHYSICS

Comprehensive dosimetric characterization of novel silicon carbide detectors with UHDR electron beams for FLASH radiotherapy

Giuliana Milluzzo[1] | **Marzio De Napoli**[1] | **Fabio Di Martino**[2,3,4] | **Antonino Amato**[5,6] | **Damiano Del Sarto**[2,3] | **Maria Cristina D'Oca**[1,7] | **Maurizio Marrale**[1,6] | **Luigi Masturzo**[2,3,8] | **Elisabetta Medina**[9,10] | **Chinonso Okpuwe**[1,11,12] | **Jake Harold Pensavalle**[2,3,8] | **Anna Vignati**[9,10] | **Massimo Camarda**[5,13] | **Francesco Romano**[1,14]

[1]National Institute of Nuclear Physics (INFN), Catania Division, Catania, Italy

[2]Centro Pisano ricerca e implementazione clinica Flash Radiotherapy (CPFR@CISUP), Pisa, Italy

[3]Fisica Sanitaria, Azienda Ospedaliero Universitaria Pisa AOUP, Pisa, Italy

[4]National Institute of Nuclear Physics (INFN), Pisa Division, Pisa, Italy

[5]STLab srl, Catania, Italy

[6]National Institute of Nuclear Physics (INFN), Laboratori Nazionali del Sud, Catania, Italy

[7]Department of Physics and Chemistry "Emilio Segrè", University of Palermo, Palermo, Italy

[8]SIT-Sordina, Aprilia, Italy

[9]Physics Department, University of Torino, Torino, Italy

[10]National Institute of Nuclear Physics (INFN), Torino Division, Torino, Italy

[11]Physics Department, University of Catania, Catania, Italy

[12]Department of Physics, Federal University of Technology Owerri, Owerri, Nigeria

[13]SenSiC GmbH, Villigen, Switzerland

[14]Particle Therapy Research Center (PARTREC), Department of Radiation Oncology, University Medical Center Groningen, University of Groningen, Groningen, The Netherlands

Correspondence
Massimo Camarda, STLab srl, Via Anapo 53, 95126, Catania, Italy.
Email: massimo.camarda@stlab.eu

Funding information
MUR-PNRR project SAMOTHRACE, Grant/Award Number: ECS00000022; Fondazione Pisa, Grant/Award Number: 134/2021; PNRR-PNC project ANTHEM, Grant/Award Number: PNC0000003; CSN5 of the INFN with the FRIDA national project

Abstract

Background: The extremely fast delivery of doses with ultra high dose rate (UHDR) beams necessitates the investigation of novel approaches for real-time dosimetry and beam monitoring. This aspect is fundamental in the perspective of the clinical application of FLASH radiotherapy (FLASH-RT), as conventional dosimeters tend to saturate at such extreme dose rates.

Purpose: This study aims to experimentally characterize newly developed silicon carbide (SiC) detectors of various active volumes at UHDRs and systematically assesses their response to establish their suitability for dosimetry in FLASH-RT.

Methods: SiC PiN junction detectors, recently realized and provided by STLab company, with different active areas (ranging from 4.5 to 10 mm^2) and

thicknesses (10–20 μm), were irradiated using 9 MeV UHDR pulsed electron beams accelerated by the ElectronFLASH linac at the Centro Pisano for FLASH Radiotherapy (CPFR). The linearity of the SiC response as a function of the delivered dose per pulse (DPP), which in turn corresponds to a specific instantaneous dose rate, was studied under various experimental conditions by measuring the produced charge within the SiC active layer with an electrometer. Due to the extremely high peak currents, an external customized electronic RC circuit was built and used in conjunction with the electrometer to avoid saturation.
Results: The study revealed a linear response for the different SiC detectors employed up to 21 Gy/pulse for SiC detectors with 4.5 mm^2/10 μm active area and thickness. These values correspond to a maximum instantaneous dose rate of 5.5 MGy/s and are indicative of the maximum achievable monitored DPP and instantaneous dose rate of the linac used during the measurements.
Conclusions: The results clearly demonstrate that the developed devices exhibit a dose-rate independent response even under extreme instantaneous dose rates and dose per pulse values. A systematic study of the SiC response was also performed as a function of the applied voltage bias, demonstrating the reliability of these dosimeters with UHDR also without any applied voltage. This demonstrates the great potential of SiC detectors for accurate dosimetry in the context of FLASH-RT.

KEYWORDS
dosimetry, FLASH radiotherapy, silicon carbide, UHDR

1 | INTRODUCTION

Several preclinical in-vivo studies have shown that the irradiation of tumors with ultra high dose rate (UHDR) beams with an average dose rate of more than 40 Gy/s leads to similar tumor control probability (TCP) as conventional radiotherapy (CONV-RT) while minimizing toxicity and complications to the surrounding healthy tissues (Normal tissue complication probability, NTCP).[1–4] Despite several experimental findings, the radiobiological effect known as FLASH effect, is not yet deeply understood. However, there are some hypotheses that could explain the enhanced sparing effect in normal cells with UHDR beams, such as the correlation with induced oxygen depletion in normal tissues[5] and the role of the immune system.[6,7] The FLASH effect was observed by delivering a single or few fractions of several Gy (>8 Gy) in a total irradiation time of 100−200 ms. Such conditions pose new technological challenges for beam dosimetry and real-time monitoring,[8–11] in the perspective of the clinical translation of FLASH-RT. Commercially available reference dosimeters currently recommended by the international protocols for reference dosimetry,[12] such as ionization chambers (IC), are affected by significative ion recombination and a noticeable decreased ion collection efficacy for a delivered dose per pulse (DPP) > 0.1 Gy.[13,14] So far, some promising approaches were explored to solve such issues with IC, such as designing innovative structures with thinner gap (<0.5 mm)[15] or investigating alternative gas mixtures and pressures which drastically decrease the ion recombination.[16] The possibility of still using commercially available ionization chambers by developing new analytical methods to calculate the saturation factor and correct the IC response for the ion recombination was also explored. However, these methods seem to work for DPP values lower than 0.5 Gy.[17,18] Passive detectors, such as radiochromic films[19] and alanine dosimeters[20] which have proven to be dose-rate independent, are also widely employed at UHDRs. However, their use requires a post-processing time-consuming analysis that makes them unsuitable for clinical practice and Quality Assurance (QA) procedures.

Recently, in terms of active detectors, the use of small portable calorimeters for reference dosimetry with UHDR beams was investigated by several groups, including Primary Standard Metrology Laboratories, where this accurate technique is mainly developed. This technology, typically quite complex for dosimetry at primary standard level at conventional dose rates, is becoming popular for FLASH radiotherapy. Indeed, in this case it is possible to take advantage of the nearly instantaneous dose delivery occurring at UHDRs, which leads to a nearly instantaneous increase of the temperature in the calorimeter core. As a result, heat transfer from/to the core with the external environment can be neglected, providing the opportunity for much less complex, and therefore more compact and portable, systems based on calorimetry.[21–24]

Alternative promising approaches are based on active solid-state detectors to real-time measure the delivered dose, as in the case of the diamond and Silicon

based detectors.[25] Small size micro-diamond Schottky diode detectors realized at Rome Tor Vergata University and commercialized by the PTW Freiburg have been recently optimized for their use in FLASH radiotherapy by modifying both the geometry and the doping quantity. The promising results reported by M. Marinelli et al.,[26] have demonstrated the suitability of such devices for their use with UHDR electron beams, thanks to their linear response with DPP up to 25 Gy/pulse, although further studies need to be carried out to systematically investigate the radiation damage and long-term stability.

On the other hand, silicon carbide (SiC) based detectors have recently been identified as a promising alternative active dosimeter at UHDRs.[27,28]

SiC detectors present many interesting properties and are widely used for radiation detection.[29] Thanks to their high breakdown voltage, they can work with high electric fields. Their resistance to high temperature enables their usage also in extreme environments, including those with elevated radiation levels. Moreover, the wide bandgap (3.23 eV), the e-h pair production energy (7.6-8.4 eV) and strong covalence bounds make them highly resistant to ionizing radiation, especially when compared to Silicon detectors. They maintain good performances and stability even when exposed to high levels of radiation.[27]

In this study, we aim to dosimetrically characterize newly developed SiC detectors having different active volumes with UHDR low energy electron beams accelerated at the Centro Pisano for FLASH Radiotherapy (CPFR). Thanks to the unique design of the available LINAC, a systematic and independent variation of the beam parameters such as the input beam current and the field size, was possible. In contrast to the irradiations performed in the previous study, the LINAC installed at CPFR allows for characterizations in terms of both dose per pulse and instantaneous dose rate at fixed field size. Moreover, for the first time, the study of the SiC detector response was extended up to higher dose per pulse and new solutions were established to avoid saturation of the electronics.

The presented results demonstrate that the SiC detectors have a charge response independent of the DPP and instantaneous dose rate, up to the most extreme regimens used for FLASH radiotherapy. The obtained results pave the way towards a clinical translation of this promising technology and its usage for UHDR beam dosimetry.

2 | MATERIALS AND METHODS

A set of measurements with UHDR electron pulsed beams have been performed to first enable the investigation of the dependence of the different SiC models with the external applied bias voltage at a fixed incident beam current and DPP of 1.5 Gy and a pulse duration of 4 μs. The collected charge within the different SiC detectors at the operational voltage fixed according to the response-voltage curve was, then, investigated varying the DPP and the instantaneous dose rate within the single electron pulse. The beam size was also varied using a 30, 40, 100 mm diameter applicator and the uncollimated beam. A fixed pulse width of 4 μs was set for all the measurements. This made it possible to investigate the dose-rate independence of the SiC detectors. The details of the materials and methods used for the experimental tests are described in the following sections.

2.1 | SiC detectors

The SiC detectors used for this systematic characterization have been produced by the STLab start-up.[30] They are based on PIN junctions, where a 0.3 um p+ high doped layer ($N_A = 10^{19}$ cm^{-3}) is placed on top of a *n*-low doped layer ($N_D = 8\ 10^{13}$ cm^{-3}) with a thickness that can range from 200 nm up to 100 μm (Figure 1a). The two layers are located on top of a $n+$ 370 μm thick substrate ($N_D = 5\ 10^{18}$ cm^{-3}). Different active areas have been realized from 1 × 1 mm^2 up to 10 × 10 mm^2 (with the possibility of having both squared and circular shapes), and from 0.2 μm up to 20 μm active thicknesses.

Moreover, thanks to a recent patent achieved by the STLab company, a new configuration of SiC detectors can be also realized removing the 370 μm *n*+ thick substrate through doping selective electrochemical etching.[31] In this configuration, called "free-standing membranes", the *n*+ bulk substrate is removed from the sensitive area, leading to ultra-thin and highly transparent devices.

As it is shown in Figure 1, the SiC detectors were glued on a ceramic PCB (Printed Circuit Board): the bondings between the detector electrode and the Au pads used to collect the produced charge within the SiC active layer and supply the bias voltage, have been realized at the INFN Catania Division. A connector is then placed in contact with the Au pads to read the signal and apply the reverse bias voltage to the detector.

The details of the detectors used in this study are listed in Table 1, indicating the active area and thickness and the calculated geometrical capacitance. The SiC detectors were named using the following scheme*: S[active area in mm^2]–[thickness in um]*. For the characterization discussed in this work, only the standard SiC detectors provided with the bulk substrate have been employed.

2.2 | The readout system

The charge collected at the SiC active layer was measured with a Keithley 6517A electrometer, which we

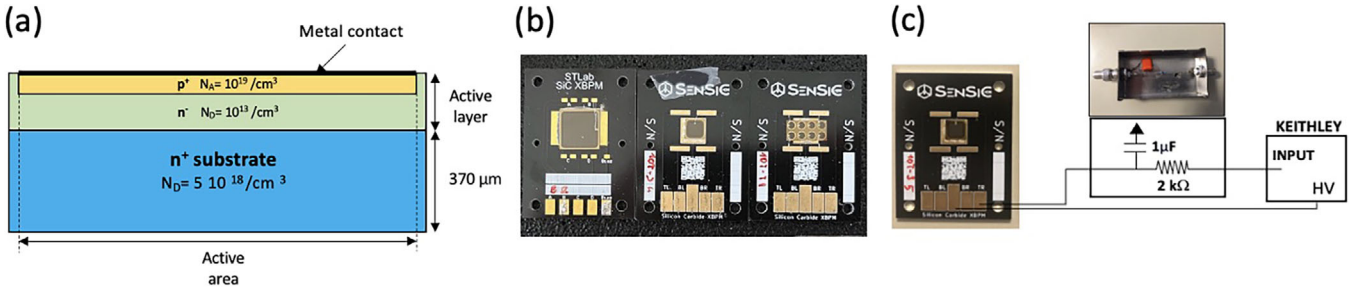

FIGURE 1 (a) Illustration of the SiC devices indicating the different layers and the substrate. (b) Photograph of the various available SiC detectors with different active areas and shapes, that is, 100 mm^2, 25 mm^2 and 4.5 mm^2 SiC detectors. (c) The RC circuit realized and used to collect and store the charge produced within the SiC active layer.

TABLE 1 Table of the SiC detectors employed in this study.

Name	Active area	Thickness	Capacitance (geometrical)
S100-10	100 mm^2 (10 × 10 mm^2)	10 µm	1.017 nF
S25-10	25 mm^2 (5 × 5 mm^2)	10 µm	254.4 pF
S4.5-10	4.5 mm^2 (1.2 mm radius)	10 µm	45.79 pF
S25-20	25 mm^2 (5 × 5 mm^2)	20 µm	138.3 pF

also used to apply the bias voltage to the detectors. As specified by the manufacturer, the Keithley 6517A electrometer can measure a maximum current of 20 mA and a maximum charge of 2 µC (at the maximum selected range). These features could limit the electrometer usage at UHDRs, as observed by F. Romano et al.,[27] who reported a preliminary characterization of these newly developed SiCs with an ElectronFLASH linac providing a limited set of irradiation conditions. Indeed, very high instantaneous currents are reached, considering the extremely high produced (and collected) charge per pulse (0.5–4 us). As shown previously[27] for a DPP > 2 Gy, a charge > 1 µC is produced and collected in a 10 × 10 mm^2, 10 µm SiC detector (like the S100-10), meaning an instantaneous current of 250 mA (for 4 µs pulse duration), that is well beyond the electrometer maximum sustainable and measurable current. The result is a signal saturation entirely caused by the overflow of the electrometer and not by the detector itself, as was observed for the highest explored DPP values.[27]

To prevent such an issue in the present work, an additional external electric circuit was connected between the detector and the triaxial input of the electrometer. The circuit, shown in Figure 1c), is composed of a resistance $R = 2$ kΩ and a capacitance $C = 1$ µF that modify the temporal structure of the single electron current pulse. Once the collected charge is accumulated at the surfaces of the capacitor arms, the charge is then released and measured by the Keithley electrometer in a time interval dependent on the constant time τ of the RC circuit, which in this case was $\tau = 2$ ms. The result is that the current signal coming from the detector is broadened in time and the instantaneous peak current is reduced to a value lower than the Keithley maximum current range (20 mA). However, depending on the detector area and the expected collected charge per pulse, if multiple pulses are delivered with a certain pulse repetition frequency (PRF), the RC circuit must be properly designed: the requirement is that the duration of each single pulse increased by the presence of the RC circuit, must be still less than the time interval between one pulse and the subsequent one.

For such reason the values of the R and C used in this characterization were also chosen to allow that a maximum PRF of the accelerator of 100 Hz could be used with no overlap between two subsequent signals.

With this approach, the output signal that is read by the Keithley electrometer will have a modified current pulse shape, while the integral of the current as a function of the time, that is, the charge, is still conserved. This technique avoids any undesired modifications in the final measured charge as demonstrated by performing electronic tests with an event generator. A signal emulating the single electron pulse in terms of pulse duration (4 µs), rise time and amplitude was generated with an event generator and sent to the RC circuit. The resulting signal was then recorded with an oscilloscope and integrated in time to compare the output charge with the injected charge (integral of the input signal produced by the event generator).

2.3 | The ElectronFlash (EF) accelerator

The SiC characterization was carried out with the SIT Sordina (SIT S.p.A., Aprilia, Italy) ElectronFlash (EF) LINAC[32] installed at the CPFR in Pisa (Italy). Thanks to the experience gained by the SIT in the design of IORT (Intra Operative RadioTherapy) dedicated linacs,[33] the EF linac is based on a new concept of waveguide adopting the radial focusing technique which avoids significant X-ray leakage and allows a better control and compactness of the whole system.

Three EF machines are currently in operation: the first one is installed at Orsay Research Center of Institute Curie, the second one at the University of Antwerp, Belgium and the third one is in operation at Centro Pisano Flash RadioTherapy (CPFR) in Pisa from August 2022.[34]

In particular, the EF in use at the CPFR in Pisa has the unique capability to vary the number of electrons accelerated per pulse without altering the energy spectrum, thanks to the presence of a triode e-gun.[35] This means that the three main beam parameters to be investigated, that is, DPP, pulse duration and pulse frequency, can be varied independently, allowing for a systematic characterization of the SiC detectors by varying several beam parameters independently from one and another. Therefore, the instantaneous dose rate at the irradiation point can vary over about two orders of magnitude without changing the geometrical configuration, that is, without changing the final beam applicators, as typically done for diode e-gun machines (as the one used by Felici et al.,[34]).Electron beams of 7 and 9 MeV can be produced and accelerated, with variable DPP from conventional up to UHDR values by adjusting the electron beam current (1–100 mA). Moreover, the DPP can also be modified with the applicators, since they have both variable lengths and diameters of 10, 30, 40, 100, and 120 mm: the larger the applicator diameter the lower the DPP, at fixed electron beam current.

The LINAC was set to deliver 10 accurately characterized beam current values with no significant variation in the energy spectrum of particles that, combined with the different final diameter applicators, provide a wide range of DPP from tens of mGy up to about 20 Gy. The single pulse duration can be also varied from 0.5 μs up to 4 μs. The above-described features allow to set the dose-rate within the single pulse, that is, the instantaneous dose rate, which is one of the key parameters to investigate for the FLASH effect.

Finally, the average dose-rate can be controlled by also varying the PRF in the range between 1 and 245 Hz. Single pulse delivery can be also selected. The beam delivery is pulse-to-pulse monitored with two AC-Current Transformer (ACCT) supplied by the Bergoz company[36,37] and mounted along the Linac with the aim of measuring the beam current without any perturbation.

2.4 | Experimental setup

Different EF parameters and geometrical configurations were chosen to cover a wide range of DPP and instantaneous dose rate and to systematically characterize the detector response under conventional and UHDR conditions. Applicators with 30 mm (APP 30), 40 mm (APP 40) and 100 mm (APP 100) diameter were used, corresponding to a source-to-surface distance (SSD) of 71.8, 76.8 and 106 cm, respectively. A final measurement was carried out without the applicator, directly after the exit window. In this set of acquired data, a fixed pulse duration of 4 μs and 10 different beam current values were set for each geometric configuration.

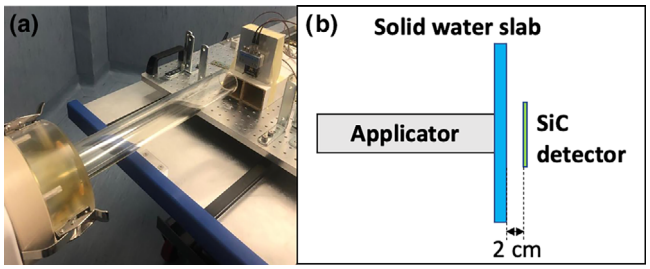

FIGURE 2 (a) Photograph of the adopted experimental setup. A final 40 mm diameter PMMA cylindrical applicator is visible together with the SiC detectors mounted in its holder. (b) Top-view scheme of the experimental setup showing the 13 mm thick solid water slab and the 2 cm air gap between the solid water slab and the detector surface, needed for the detector read-out connectors.

A photograph of the experimental setup is shown in Figure 2a (the solid water slab placed in front of the detector was removed to make the SiC detector visible for the photo), together with a schematic top view in Figure 2b.

As shown in Figure 2b, a 13 mm thick solid water slab (light blue rectangle in the Figure) was placed between the applicator and the detector surface, in contact with the applicator to place the detectors at the depth corresponding to the maximum dose deposition (RMAX) of the 9 MeV electron beam. The depth-dose distribution was previously measured for the different configurations as reported in.[35]

As can be seen in Figure 2b, for all the measurements performed with an applicator, there was a 2 cm air gap between the solid water slab and the detector surface as the space was occupied by the connectors used for the acquisition of the signals. The air gap was also added during the calibration procedure of the ACCTs with the alanine dosimeters as explained in the next sections. For the measurements performed without the applicator, the 2 cm air gap was not present as a different connector was used to bring the sample closer to the solid water slab and maximize the DPP.

For the configuration with the applicators, the detectors were placed at the center of the beam where a homogeneous dose distribution is expected.

The transversal dose profiles of the beam were measured with EBT-XD films placed at the SiC position for the different applicator configurations, that is, 30, 40, and 100 mm diameter applicators (Figure 3a) and without the applicator directly in front of the linac exit window (Figure 3b). A flat dose profile with a variation between 4% and 7% was observed for the 30, 40, and 100 mm diameter applicators. The isodose at 95% covered areas with diameters of 20, 30, and 60 mm, respectively, which ensured a homogeneous dose

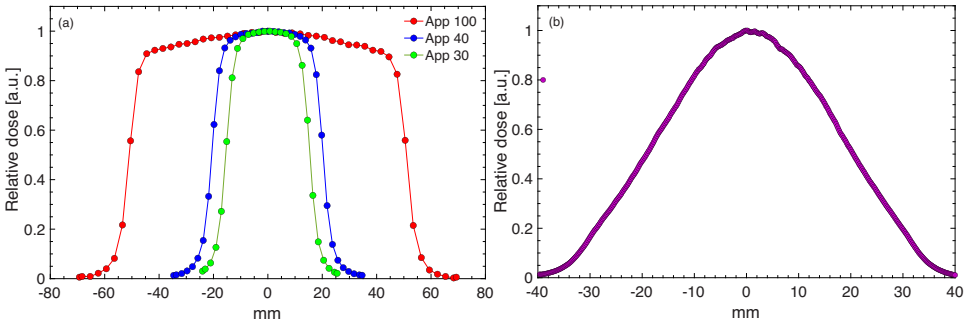

FIGURE 3 Horizontal dose profiles measured with an EBT-XD Radiochromic film at RMAX with the 30, 40, and 100 diameter applicators (a) and without any applicator (open field) (b).

delivery within 5% over the surface area of the tested SiC detectors (depending on the prototype considered, the surface area varied between 4.5 mm^2 and 1 cm^2). On the other hand, as expected, the uncollimated field showed a constant dose over a reduced area, which is about 5×5 mm^2 (Figure 3b). Because the largest DPP values are obtained with this configuration, this setup was only used for the characterization of the smallest SiC detectors, that is, the S4.5–10.

2.5 | Dose per pulse measurements

The dose delivered per pulse during the SiC irradiation was monitored through the two ACCTs placed along the LINAC. For each beam current and applicator setting, the charge response of one of the two ACCTs in terms of Monitor Units (MU) was calibrated in dose by placing a reference dosimeter at the position of the SiC detectors.

Specifically, alanine pellet dosimeters (Gamma-Service, Produktbestrahlung Germany, diameter 4.80 ± 0.04 mm, height 2.99 ± 0.02 mm, density 1.26 ± 0.02 g/cm^3) which have been proved to be dose-rate independent, were used to measure with high accuracy the dose delivered per pulse at the same position of the SiC detectors, during the ACCT calibration procedure.

The absorbed dose in the alanine pellets was extracted through EPR procedure carried out at constant room temperature, using the spectrometer ELEXSYS E580 (Bruker, Karlsruhe, Germany) operating at the X-band.[38,39] A calibration in the dose range from 2.5 to 20 Gy, was previously performed with conventional electron beams of similar energy.

For each experimental configuration, that is, fixed beam current and applicator, the calibration coefficients (Gy/MU) of the ACCT were obtained from the ratio of the DPP measured with the alanine dosimeters and the corresponding MU detected simultaneously with the ACCT.

The uncertainty of such calibration coefficients was calculated applying the error propagation method, considering the two uncertainty components: the uncertainty associated with the DPP measurement with the alanine dosimeters and the statistical uncertainty (standard deviation) of the average MU measured with the ACCT upon the repeated measurements, which was around 1% for all the measurements.

In turn, the combined total standard uncertainty of the DPP was determined considering both the type A statistical uncertainties (u_A) that is, the standard deviation of the average values of DPP obtained repeating the measurements under the same condition and the type B (u_B) uncertainties associated with the calibration in dose of the alanine pellets including the EPR procedure. In particular, the total uncertainty of the DPP, given by $u_C = \sqrt{u_A^2 + u_B^2}$, was quoted to be between 1.1% and 2% for the DPPs investigated under the different experimental configurations studied.

Finally, the total uncertainty of the calibration coefficients (in Gy/MU) calculated for each beam current setting and geometrical setup, was found to range between 1% and 2% (coverage factor $k = 1$).

The delivered dose per pulse while simultaneously irradiating the SiC detector was then evaluated by multiplying the calibration coefficients in Gy/MU for the MU detected with the ACCTs while irradiating the SiC detector.

The DPP values measured for the different experimental arrangements ranged from 0.080 ± 0.002 Gy to 4.73 ± 0.08 Gy for the APP 30, from 0.080 ± 0.002 Gy to 5.33 ± 0.07 Gy for the APP 40, 0.040 ± 0.001 Gy to 2.13 ± 0.03 Gy for the APP 100 and from 0.5 ± 0.01 Gy to 21 ± 0.34 Gy for the configuration without final applicator.

The total uncertainty of the DPP values was evaluated considering the total uncertainty associated with the calibration coefficients of the ACCT (1%–2%) and the statistical uncertainty (standard deviation) of the MU average value which was less than 1%. The total

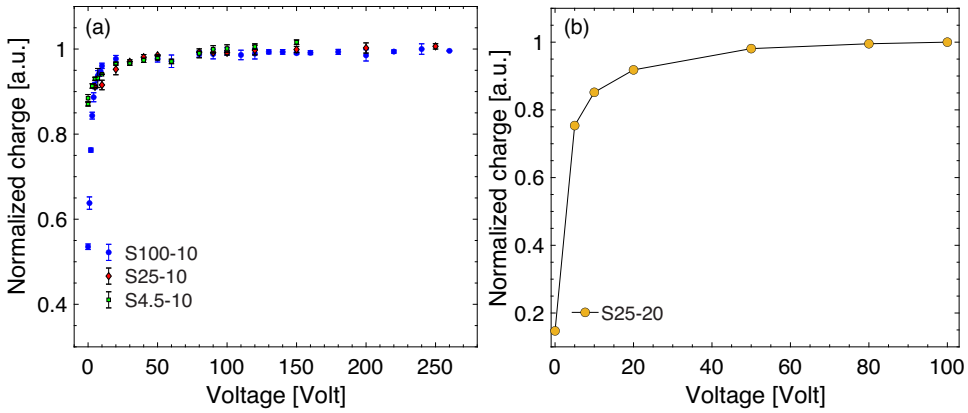

FIGURE 4 (a) Collected charge within the SiC active layer normalized to the MU measured with the in-transmission ACCT monitors as a function of the applied bias Voltage, for the S100-10, S25-10 S4.5-10 (blue circles, red diamonds, green squares) and (b) for the S25-20 SiC detector.

uncertainty of the DPP values with a coverage factor of $k = 1$ thus ranges from 1.2% to 3%.

3 | RESULTS AND DISCUSSION

As a first step of the investigation, the collected charge within the detectors active layer was measured as a function of the applied bias voltage for a fixed beam current, that is, a fixed DPP, and a pulse duration of 4 μs. In particular, the measurements were carried out using a 40 mm diameter applicator and a nominal DPP of 1.5 Gy. Figure 4a shows the collected charge with the 10 μm thick detectors having three different active areas (100, 25, 4.5 mm^2) as a function of the applied bias Voltage.

In particular, the ratio between the average charge values ($\bar{q}$) measured with the SiC detectors and the corresponding average MU detected with the ACCT ($\overline{MU}$) (single pulse), were calculated for each voltage. These values, as shown in Figure 4a, were then normalized at the maximum measured value of $\bar{q}/\overline{MU}$ for the different applied bias voltages by using the following formula:

$$\begin{aligned} &Normalized\ charge_{BIAS} \\ &= \frac{\sum_{i=1}^{3} q_i}{\sum_{i=1}^{3} MU_i}\bigg|_{BIAS} * \frac{1}{\max\left(\frac{\sum_{i=1}^{3} q_i}{\sum_{i=1}^{3} MU_i}\right)} \\ &= \frac{\bar{q}}{\overline{MU}}\bigg|_{BIAS} * \frac{1}{\max\left(\frac{\bar{q}}{\overline{MU}}\right)} \end{aligned}$$

Figure 4 also shows the corresponding standard deviation of the average values. Using the same approach, Figure 4b shows the data as a function of the bias Voltage for the 25 mm^2, 20 μm thick detector (S25-20). In this case, only a single repetition of the measurement was possible, which is the reason why for this plot no uncertainties are shown. As expected in PiN semiconductor junction-based detectors, by increasing the Voltage, the collected charge increases with the bias voltage until it reaches a nearly flat region, where the charge response is fairly independent of the bias voltage. This independence indicates that both the full depletion of the active region and the maximum charge collection efficiency are achieved.[25]

Based on the results shown in Figure 4, to study the linearity of the SiC response as a function of the DPP and the instantaneous dose-rate, the detectors S100-10, S25-10 were biased at 200 V while the detectors SB4.5-10 and SB25-20 were biased at 80 V.

Figure 5 shows the collected charge within the sB100-10 detector irradiated with a single incident electron pulse by varying the beam current within the single pulse and keeping the same pulse length at 4 μs, for each of the three different applicators (Figure 5a–c).

An overall uncertainty in the measured charge per pulse ($k = 1$) between 0.5% and 2% (not visible in Figure 5, as included within the markers) was evaluated considering the statistical error (type A) component (standard deviation) due to the measure repetition under the same experimental condition and the sensitivity of the instrument used to measure the charge.

The DPP values shown in Figures 5 and 6 along with the displayed uncertainties have been obtained following the procedure explained in Section 2.5.

As shown in Figure 5a linear response with the DPP was observed for the s100-10 detector irradiated with the different applicators. A linear fit was performed for each geometrical configuration to evaluate the linearity of the acquired data ($R^2 = 0.999$ for all the configurations). The measured charge was varying from 14 nC (DPP = 0.037 Gy, APP 100) up to 1.8 μC (DPP = 5.329 Gy, APP 40). As explained above, for a

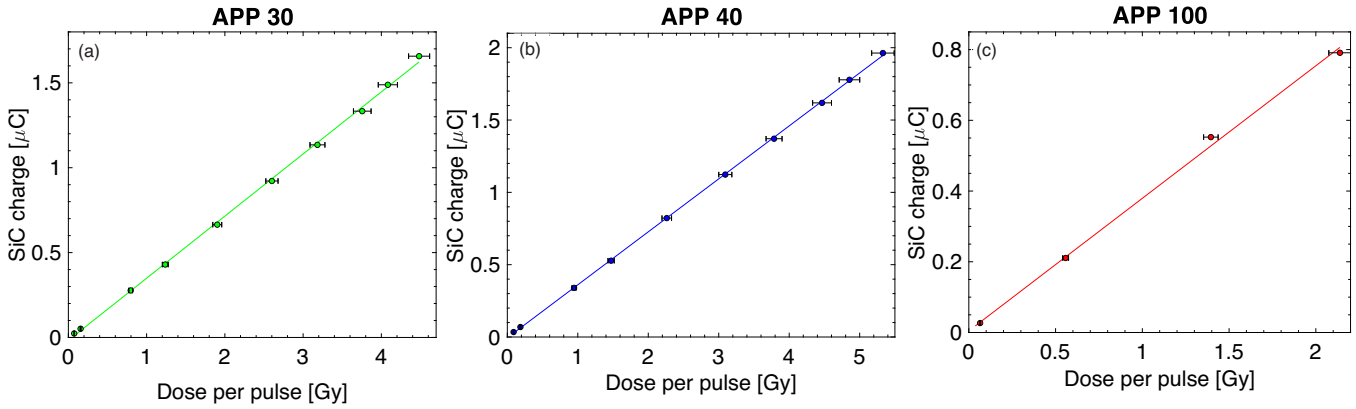

FIGURE 5 Charge response of the s100-10 SiC detector as a function of the DPP obtained with the (a) 30 (green points), (b) 40 (blue points) and (c) 100 (red points) mm diameter applicators. The linear fits are also shown.

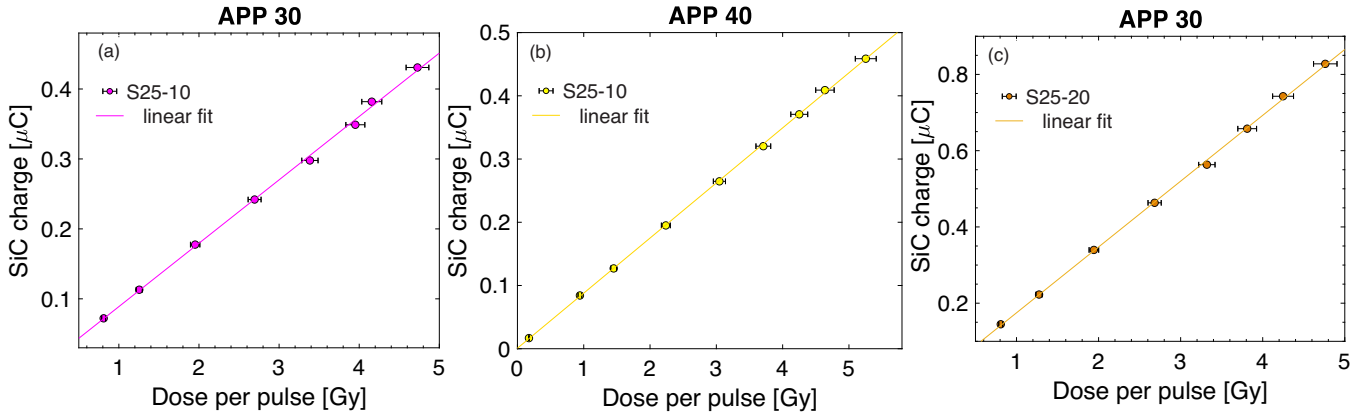

FIGURE 6 Charge response of the S25-10 SiC detector as a function of the DPP measured with the alanine dosimeters placed at the SiC position for the 30 (a) and 40 (b) mm diameter applicators and of the thicker S25-20 for the 30 mm applicator configuration (c). The linear fits are also shown.

charge per pulse exceeding 80 nC (which means a current > 20 mA within the single pulse of 4 μs), the use of a RC circuit was necessary to avoid saturating the maximum current range of the Keithley electrometer.[27]

A linear response was also observed for the S25-10 detector using the same beam current settings with the 30 and the 40 mm diameter applicators as shown in Figure 6a and b. Due to the smaller active area of the S25-10, four times smaller than the S100-10, the collected charge is proportionally smaller and varies from 160 nC (DPP = 0.17 Gy) up to 460 nC (DPP = 5.3 Gy). The charge response with the DPP of the thicker sB25-20 detector is also shown in Figure 6c) for the case of 30 mm diameter applicator. As expected, due to the thicker active layer a higher sensitivity is observed compared with the 10 μm thick detector of the same area. A linear response ($R^2 = 0.99$) is observed up to highest possible value of DPP for this configuration, that is, at 4.7 Gy/pulse and a charge measured per pulse of about 800 nC.

To quantify possible dependences of the DPP from the different field size obtained with the specific applicators, all the collected data with the S100-10 and S25-10 detectors shown in Figures 5 and 6 have been collected and overlapped in the same plot in Figure 7. As shown, for both the detectors, the charge response for a specific DPP obtained with a different applicator configuration is independent of the specific geometrical configuration. This result also confirms the reliability and accuracy of the performed dose measurements and the robustness of the data analysis. Therefore, a unique linear fit for all the data acquired can be also calculated as displayed in Figure 7.

Table 2 shows the fitting parameters, along with the corresponding uncertainties, retrieved linearly fitting (a^*x+b) the data shown in Figures 5 and 6, the parameters obtained by linearly fitting the all data for a specific detector (all the applicator configurations) and shown in Figure 7 are also reported, revealing a discrepancy for the parameter a, as respect to the parameter a of the

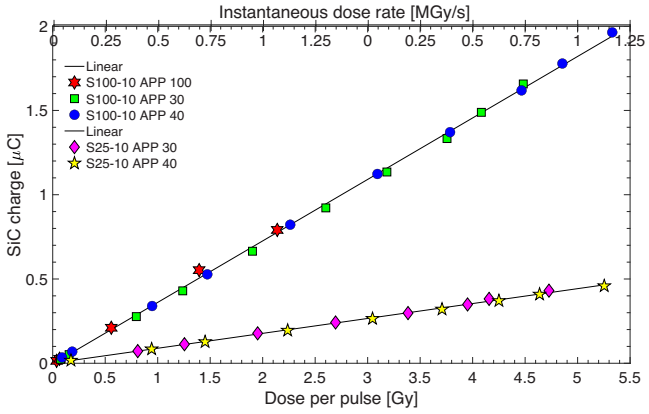

FIGURE 7 Collected charge for the S100-10 and S25-10 detectors as a function of the DPP measured with the alanine dosimeters (*x* axis) and the average instantaneous dose rate (*y* axis) obtained with different applicator setup.

TABLE 2 Fitting parameters for the data shown in Figures 5–7.

SiC detector	APP	a [μC/Gy]	b [Gy]
sB100_10	30	0.365 ± 0.003	−0.016 ± 0.010
	40	0.366 ± 0.001	−0.005 ± 0.005
	100	0.368 ± 0.009	0.004 ± 0.011
	All	0.364 ± 0.002	−0.003 ± 0.005
sB25_10	30	0.090 ± 0.001	−0.002 ± 0.004
	40	0.087 ± 0.001	−0.008 ± 0.001
	All	0.088 ± 0.001	−0.001 ± 0.003

individual linear fits (Figures 5 and 6), ranging from 0.3% up to a maximum of 2%.

Moreover, the average values of the intra-pulse instantaneous dose-rates corresponding to the different explored DPPs were easily calculated by considering the fixed pulse length of 4 us and the dose delivered for this pulse duration (as DPP/4 μs). The results are depicted on the top axis of Figure 7 and show instantaneous dose rates varying from 0.01 MGy/s up to 1.37 MGy/s for all the data acquired with the S100-10 and S25-10 detectors.

To extend the linearity studies up to highest values of DPP and corresponding instantaneous dose-rate that the EF linac can produce, the smaller S4.5-10 detector was placed at a few mm after the exit window of the ElectronFLASH linac, without any applicator, still at RMAX (i.e., after 13 mm thick solid water slab) and without any air gap. This arrangement maximizes the dose delivered per pulse at the center of the beam and the use of the smallest area detector enabled to get a good dose homogeneity over the total detector surface even in this peculiar configuration (Figure 3b).

Moreover, considering that much larger dose per pulse is delivered for this specific configuration, larger areas SiC would have also implied a produced and then collected charge within the active area well beyond the maximum measurable charge with the Keithley electrometer.

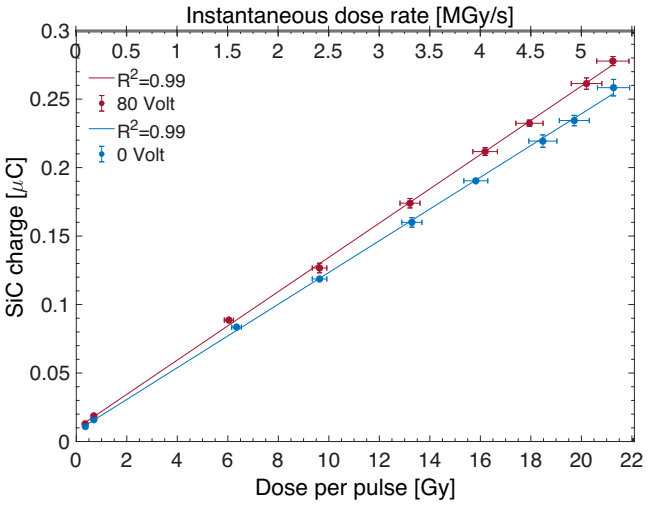

FIGURE 8 Measured charge with the S4.5-10 detector at 80 V external applied bias as a function of the DPP (red points) and the corresponding instantaneous dose rate (top axis). A comparison of the collected charge with the same detector at 0 V external applied bias is also reported (blue points).

TABLE 3 Calibration coefficients in Gy/μC for the SiC detectors used in the characterization.

SiC detector	Gy/μC
S100-10	2.75 ± 0.06
S25-10	11.4 ± 0.25
S25-20	5.81 ± 0.11
S4.5-10 (80 V)	83.33 ± 2.63
S4.5-10 (0 V)	90.9 ± 2.87

Specifically, DPP values varying from 0.5 Gy up to 21 Gy and an average instantaneous dose rate (top axis in Figure 8) up to 5.5 MGy/s were measured for this configuration. For this measurement, 80 V external bias was applied to the S4.5-10 detector.

As shown in Figure 8, the experimental data exhibit a linear trend ($R^2 = 0.99$) also at these extreme regimes and the charge detected at the maximum achievable DPP of 21 Gy was 280 nC. The charge response of the S4.5-10 detector was also studied repeating the same irradiations without applying the bias voltage, as shown in Figure 8. As it can be seen, the response is still linear although, as expected, a reduced sensitivity in terms of collected charge can be observed at 0 V with respect to the 80 V case. The reduction in the detected charge can be attributed to two factors: the partial depletion of the active layer that leads to a reduced produced charge (the active thickness being less than 10 μm) and the suboptimal collection of charges occurring without any external electric field.

TABLE 4 Comparison of the normalized values of DPP measured with the S100-10, S25-10 and the fD for four different nominal DPP and 40 mm applicator.

Nominal DPP (Gy)	S100-10 (cGy/MU)	S25-10 (cGy/MU)	fD (cGy/MU)	Discrepancy S100-10/fD (%)	Discrepancy S25-10/fD (%)
2.2	2.719 ± 0.05	2.642 ± 0.05	2.642 ± 0.08	2.8%	0.01%
3	2.742 ± 0.05	2.635 ± 0.05	2.662 ± 0.08	2.9%	–1%
3.7	2.729 ± 0.05	2.619 ± 0.05	2.657 ± 0.07	2.7%	–1.4%
5.4	2.735 ± 0.05	2.648 ± 0.05	2.672 ± 0.07	2.3%	–0.9%

This study is particularly important to rule out potential electron-hole recombination effects within the active layer. Especially at high DPP values, corresponding to a high fluence of incident particles, and in the absence of an external electric field that accelerates charge collection, possible saturation effects could be present. Figure 8 demonstrates that although less charge is collected at 0 Volts, the charge response to the DPP remains linear up to the maximum DPP of 21 Gy/pulse and for the considered DPP range. This result indicates that if for some reasons the considered SiC detector must be used with no external applied bias, its response is still reliable at these extreme DPP values, typical of FLASH radiotherapy applications.

The resulting calibration coefficients in terms of Gy/μC for the S100-10, S25-10, S4.5-10 and S25-20 have been calculated and reported in Table 3 to emphasize the different sensitivities of the SiC detectors of different active volume to the dose. The uncertainties have been estimated considering the uncertainty in the slope of the linear fits shown in Figures 7 and 8 and the uncertainties resulted from the calibration procedure.

Although these SiC detectors are still prototypes, considering we are engineering them for a possible usage as reliable field dosimeters in FLASH radiotherapy, a cross comparison was carried out with the PTW FLASH diamond (fD) detector.[40] For this comparison, the 40 mm applicator was used, again using the RMAX (13 mm water equivalent depth) as point of measurement in terms of longitudinal dose distribution. In particular, the fD was placed at the measurement position using a cylindrical PMMA 120 mm diameter phantom and it was connected to a PTW UNIDOS E (PTW-Freiburg, Germany) electrometer to measure the collected charge per pulse. A calibration factor of 3.99 Gy/nC was used for the fD, as reported for dedicated calibration procedures. A total overall uncertainty of 3% can be considered for the fD calibration factor.

The dose values estimated with the calibrated S100-10 and S25-10 SiC detectors and the fD normalized to the delivered monitor units recorded with the ACCT during each irradiation are reported in Table 4 for four beam current settings (i.e., four different nominal DPP values). The corresponding percentage difference between the values obtained with the two SiC detector models and the fD are also reported, showing a discrepancy within 3% for the case of the larger S100-10 SiC detectors and within 1.5% for the comparison with the smaller S25-10.

4 | CONCLUSIONS

The charge response of novel SiC detectors was investigated in a wide range of DPP and instantaneous dose rate using the 9 MeV UHDR pulsed electron beams accelerated by the triode gun ElectronFLASH linac installed at the CPFR in Pisa. This unique accelerator, thanks to the triode gun, allows for the independent variation of all the beam parameters, like the current within a single electron pulse and the beam size at the irradiation point.

In particular, the produced charge per single pulse within the SiC detectors with active area of 4.5, 25, and 100 mm^2 and thicknesses of 10 and 20 μm was measured with a Keithley 6517A electrometer, varying the dose delivered per pulse, that is, varying both the beam current and the final field size.

To prevent the saturation of the Keithley electrometer used for the charge measurement, which was observed in a previous study,[24] a dedicated external RC circuit was coupled to the electrometer to correctly and accurately measure the produced charge within the SiC active layer.

Alanine pellet dosimeters previously calibrated were used as reference dosimeters during the calibration procedure of the beam monitoring system, that is, the ACCT mounted along the LINAC.

The results show a linear response up to approximately 5 Gy/pulse for all the detectors (S100-10, S25-10, S25-20) tested with a final applicator of 30, 40, and 100 mm diameter.

Moreover, for the smallest SiC detector, that is, the S4.5-10, which was tested without any final applicator, the linear response was observed up to the maximum achievable DPP in this condition of 21 Gy/pulse and a maximum instantaneous dose rate of 5.5 MGy/s. Additionally, the possibility of using SiC detectors under UHDR electron beams without applying external bias was also successfully investigated, showing that a linear response is still preserved, with an expected reduced sensitivity.

Finally, the resulting calibration coefficients were calculated for all the SiC detectors of different area and thickness. In particular, the dose values measured with the calibrated S100-10 and S25-10 SiC detectors were compared to the ones obtained with the calibrated PTW Flash diamond detector irradiated in the same conditions, that is, 40 mm diameter applicator and four different beam current settings. The results revealed a good agreement with the fD, within the 3% and 1.5% for the S100-10 and S25-10 SiC detectors, respectively. The successful comparison with the fD is significant as it demonstrates the reliability of the calibration procedure realized for this characterization and the suitability of the these newly developed SiC detectors for dosimetry for FLASH-RT.

Currently, the possibility of performing real-time measurements with SiC, that is, measuring the pulse shape with high temporal resolution within each single pulse, is being investigated. This includes the measurement of the possible variations of the instantaneous dose rate within the single electron pulse, which is also essential for advancing our understanding of FLASH-RT and its potential benefits in clinical applications.

The establishment of this new technology for dosimetry at UHDRs, as carried out in this work, paves the way towards alternative approaches that can address some issues still not fully solved in terms of real-time beam monitor and dosimetry for FLASH-RT. In particular, the high radiation hardness of these detectors together with the possibility of producing larger area sensors with linear responses at UHDRs, as demonstrated in this work, may allow, for instance, two-dimensional relative dose measurements for one single shot, addressing radiation protection issues coming from the scanning lateral and longitudinal profiles with one single detector.

ACKNOWLEDGMENTS

The presented work was performed within the framework of the national project FLASH Radiotherapy with hIgh Dose-rate particle beAms (FRIDA) and was financed by the National Scientific Committee 5 (CSN5) of the INFN. This work was also funded by the National Plan for NRRP Complementary Investments (PNC, established with the decree-law May 6, 2021, n. 59, converted by law n. 101 of 2021) in the call for the funding of research initiatives for technologies and innovative trajectories in the health and care sectors (Directorial Decree n. 931 of 06-06-2022)—project n. PNC0000003—AdvaNced Technologies for Human-centrEd Medicine (project acronym: ANTHEM). This work reflects only the authors' views and opinions, neither the Ministry for University and Research nor the European Commission can be considered responsible for them. This work has been partially funded by European Union (NextGeneration EU), through the MUR-PNRR project SAMOTHRACE (ECS00000022). We also thank Fondazione Pisa for funding CPFR with the grant prog. n. 134/2021. We kindly thank the staff of Tecnologie Avanzate service and of the mechanical workshop of the INFN-CT division, namely Nunzio Giudice, Antonio Grimaldi, Francesco Librizzi, Domenico Sciliberto and Antonio Rapicavoli for their valuable support in the preparation of the detectors for the experimental characterization.

CONFLICT OF INTEREST STATEMENT

M. Camarda is the STlab founder. J. Pensavalle is SIT S.p.A. employee.

REFERENCES

1. Favaudon V, Caplier L, Monceau V, et al. Ultrahigh dose-rate FLASH irradiation increases the differential response between normal and tumor tissue in mice. *Sci Transl Med*. 2014;6(245):245ra93.
2. Montay-Gruel P, Bouchet A, Jaccard M, et al. X-rays can trigger the FLASH effect: ultra-high dose-rate synchrotron light source prevents normal brain injury after whole brain irradiation in mice. *Radiother Oncol*. 2018;129(3):582-588.
3. Vozenin MC, De Fornel P, Petersson K, et al. The advantage of FLASH radiotherapy confirmed in mini-pig and cat-cancer patients. *Clin Cancer Res*. 2019;25(1):35-42.
4. Montay-Gruel P, Corde S, Laissue JA, et al. FLASH radiotherapy with photon beams. *Med Phys*. 2022;49(3):2055-2067.
5. Esplen N, Mendonca MS, Bazalova-Carter M. Physics and biology of ultrahigh dose-rate (FLASH) radiotherapy: a topical review. *Phys Med Biol*. 2020;65(23):23TR03.
6. Wirsdörfer F, Jendrossek V. The role of lymphocytes in radiotherapy-induced adverse late effects in the lung. *Front Immunol*. 2016;7:591.
7. Ni W, Xiao Z, Zhou Z, et al. Severe radiation-induced lymphopenia during postoperative radiotherapy or chemoradiotherapy has poor prognosis in patients with stage IIB-III after radical esophagectomy: a post hoc analysis of a randomized controlled trial. *Front Oncol*. 2022;12:936684.
8. Subiel A, Moskvin V, Welsh GH, et al. Challenges of dosimetry of ultra-short pulsed very high energy electron beams. *Physica Med*. 2017;42:327-331.
9. Romano F, Bailat C, Jorge PG, Lerch MLF, Darafsheh A. A. Ultra-high dose rate dosimetry: challenges and opportunities for FLASH radiation therapy. *Med Phys*. 2022;49:4912-4932.
10. Vignati A, Giordanengo S, Fausti F, et al. Beam monitors for tomorrow: the challenges of electron and photon FLASH RT. *Front Phys*. 2020;8:375.
11. Subiel A, Romano F. Recent developments in absolute dosimetry for FLASH radiotherapy. *Br J Radiol*. 2023;96(1148):20220560.
12. Petersson K, Jaccard M, et al. High dose-per-pulse electron beam dosimetry—A model to correct for the ion recombination in the advanced Markus ionization chamber. *Med Phys*. 2017;44:1157-1167.
13. McManus M, Romano F, Lee ND, et al. The challenge of ionization chamber dosimetry in ultra-short pulsed high dose-rate very high energy electron beams. *Sci Rep*. 2020;10(1):9089.
14. International Atomic Energy Agency. Absorbed dose determination in external beam radiotherapy; *Technical Reports Series No. 398*; IAEA: 2001.
15. Gómez F, Gonzalez-Castaño DM, Fernández NG, et al. Development of an ultra-thin parallel plate ionization chamber for dosimetry in FLASH radiotherapy. *Med Phys*. 2022;49:4705-4714.
16. Di Martino F, Del Sarto D, Giuseppina Bisogni, et al. A new solution for UHDP and UHDR (Flash) measurements: theory and conceptual design of ALLS chamber. *Phys Med*. 2022;102:9-18.

17. Di Martino F, Giannelli M, Traino AC, Lazzeri M. Ion recombination correction for very high dose-per-pulse high-energy electron beams. *Med Phys*. 2005;32:2204-2210.
18. Di Martino F, Del Sarto D, Barone S, et al. A new calculation method for the free electron fraction of an ionization chamber in the ultra-high-doseper-pulse regimen. *Phys Med*. 2022;103:175-180.
19. Jaccard M, Petersson K, Buchillier T, et al. High dose-per-pulse electron beam dosimetry: usability and dose-rate independence of EBT3 Gafchromic films. *Med Phys*. 2017;44:725-735.
20. Marrale M, Castronovo ERA, Collura G, et al. Alanine/EPR dosimetry for ultra-high dose rate beams used for flash radiotherapy. *Physica Med*. 2023a;115:102701.
21. Palmans H, Thomas R, Simon M, et al. A small-body portable graphite calorimeter for dosimetry in low-energy clinical proton beams. *Phys Med Biol*. 2004;49:3737-3749.
22. Bourgouin A, Keszti F, Schnfeld AA, et al. The probe-format graphite calorimeter, aerrow, for absolute dosimetry in ultrahigh pulse dose rate electron beams. *Med Phys*. 2022;49:6635-6645.
23. Bass GA, Shipley DR, Flynn SF, Thomas RAS. A prototype low-cost secondary standard calorimeter for reference dosimetry with ultra-high pulse dose rates. *Br J Radiol*. 2023;96:20220638.
24. McCallum S, Lee N, Milluzzo G, et al. Proof-of-principle of absolute dosimetry using an absorbed dose portable calorimeter with laser-driven proton beams. *Appl Sci*. 2023;13(21):11894.
25. Vignati A, Giordanengo S, Fausti F, et al. Beam monitors for tomorrow: the challenges of electron and photon FLASH RT. *Front Phys*. 2020;8(375):26.
26. Marinelli M, Felici G, Galante F, et al. Design, realization, and characterization of a novel diamond detector prototype for FLASH radiotherapy dosimetry. *Med Phys*. 2022;49(3):1902-1910.
27. Romano F, Milluzzo G, Di Martino F, et al. First characterization of novel silicon carbide detectors with ultra-high dose rate electron beams for FLASH radiotherapy. *Appl Sci*. 2023;13(5):2986.
28. Medina E, Sangregorio E, Crnjac A, et al. Radiation hardness study of Silicon Carbide sensors under high temperature proton beam irradiations. *Micromachines*. 2022;14:166.
29. De Napoli M. SiC detectors: a review on the use of silicon carbide as radiation detection material. *Front Phys*. 2022;10:898833. In.
30. STLab srl, (Catania, Italy). 2020. Available online: https://www.stlab.eu (accessed on 14 February 2023)
31. Nid SA, Tsibizov A, Ziemann T, et al. Silicon carbide X-ray beam position monitors for synchrotron applications. *J Synchrotron Radiat*. 2019;26:28.
32. S.I.T.—Sordina IORT Technologies, S.p.A. Available online: https://www.soiort.com (accessed on 14 February 2023)
33. Di Martino F, Barca P, Barone S, et al. FLASH radiotherapy with electrons: issues related to the production, monitoring and dosimetric characterization of the beam. *Front Phys*. 2020;8:570697.
34. Felici G, Barca P, Barone S, et al. Transforming an IORT linac into a FLASH research machine: procedure and dosimetric characterization. *Front Phys*. 2020;8:374.
35. Di Martino F, Del Sarto D, Bass G, et al. Architecture, flexibility and performance of a special electron linac dedicated to Flash radiotherapy research: electronFlash with a triode gun of the centro pisano flash radiotherapy (CPFR). *Front Phys*. 2023;11:1268310.
36. https://www.bergoz.com/products/acct/
37. Oesterle R, Gonçalves Jorge P, Grilj V, et al. Implementation and validation of a beam-current transformer on a medical pulsed electron beam LINAC for FLASH-RT beam monitoring. *J Appl Clin Med Phy*. 2021;22(11):165-171. 1–7.
38. Marrale M, Carlino A, Gallo S, et al. EPR/alanine dosimetry for two therapeutic proton beams. *Nuclear Instruments and Methods in Physics Research, Section B: Beam Interactions with Materials and Atoms*. Elsevier; 2016:96-102.
39. Marrale M, Brai M, Gennaro, et al. Improvement of the LET sensitivity in ESR dosimetry for photons and thermal neutrons through gadolinium addition. *Radiat Meas*. 2007;42:1217-1221.
40. https://www.ptwdosimetry.com/en/products/flashdiamond-detector

How to cite this article: Milluzzo G, De Napoli M, Di Martino F, et al. Comprehensive dosimetric characterization of novel silicon carbide detectors with UHDR electron beams for FLASH radiotherapy. *Med Phys*. 2024;1-12. https://doi.org/10.1002/mp.17172